Synthesis and characterization of mixed-valent complexes containing the Rh_2^{5+} core. X-ray crystal structure of $[Rh_2(form)_4(H_2O)]O_2CCF_3$ (form = *N,N'*-di-*p*-tolylformamidinate anion)

Giuseppe Bruno*, Sandra Lo Schiavo, Giuseppe Tresoldi, Pasquale Piraino*
Dipartimento di Chimica Inorganica e Struttura Molecolare, Università di Messina, 98010 Messina (Italy)

and Lodovico Valli
Dipartimento di Scienza dei Materiali, Università di Lecce, 73100 Lecce (Italy)

(Received December 4, 1991)

Abstract

The chemical oxidation of the Rh_2^{4+} formamidinate derivative $Rh_2(form)_4$ (form = *N,N'*-di-*p*-tolylformamidinate) with the appropriate silver salts leads to the formation of the paramagnetic complexes $[Rh_2(form)_4(H_2O)]X$ ($X = CF_3COO$ (**1**), NO_3 (**2**)). The complexes were characterized by EPR spectroscopy and X-ray analysis. The EPR spectra in frozen solution consist of two or three absorption lines. The low-field one (or two) is unresolved while the high-field one is split into a triplet. The pattern is interpreted in terms of hyperfine magnetic interaction between the unpaired electron and two equivalent ^{103}Rh nuclei ($I = 1/2$). Complex **1** crystallizes in the tetragonal *P4/ncc* space group, with $a = 14.101(2)$, $C = 29.235(3)$ Å, $V = 5813.0(4)$ Å^3, $Z = 4$ and $D_{calc} = 1.24$ g cm^{-3}. The mono-electron oxidation does not cause appreciable variation of the structural parameters of the radical species with respect to those of the parent neutral complexes. The only detectable effect is a more favourable orientation of the tolyl group attached to N(2) which allows the axial coordination of a water molecule. The oxidation results also in a slight lengthening of the Rh–Rh bond distance (2.452(2) Å) rather than shortening as expected on simple MO grounds.

Introduction

Recently we reported the synthesis, electrochemical studies, PE spectra and DV-Xα calculations on the Rh_2^{4+} complexes $Rh_2(form)_4$ and $Rh_2(form)_2(O_2CCF_3)_2(H_2O)_2$ (form = *N,N'*-di-*p*-tolylformamidinate) [1]. The UV photoelectron spectra and DV-Xα calculations evidenced progressive destabilization of all valence levels on going from $Rh_2(form)_2(O_2CCF_3)_2$ to $Rh_2(form)_4$. Furthermore cyclic voltammetry studies on both the complexes showed two subsequent one-electron reversible or quasi-reversible anodic processes and of the two electrogenerable products only the mixed-valence Rh(II)Rh(III) species are quite stable while the Rh(III)Rh(III) derivatives are stable only for the short time of cyclic voltammetry [2, 3]. These findings turned our attention to the prospect of synthesizing mixed-valent Rh_2^{5+} complexes by chemical oxidation of the above-mentioned formamidinate derivatives with silver salts.

Herein we report, as preliminary results of this investigation, the synthesis and the EPR features of the mixed-valence complexes $[Rh_2(form)_4(H_2O)]X$ ($X = CF_3COO$ (**1**), NO_3 (**2**)). We report also the X-ray analysis of complex **1** which uncovers another example of Rh_2^{4+} complex which does not fall into the pattern of expected metal–metal bond distance changes.

Experimental

The complex $Rh_2(form)_4$ was obtained by a literature procedure [3]. Other reagents and solvents were used as received. IR spectra were recorded with a Perkin-Elmer 783 instrument. EPR spectra were measured by using a Bruker SR 200D spectrometer. Elemental analyses were performed by the Microanalytical Laboratory of the Organic Chemistry Institute of Milan, Italy and Analytische Laboratorien Malissa and Reuter, Elbach, FRG.

Synthesis of $[Rh_2(form)_4(H_2O)]O_2CCF_3$ (1)

$Rh_2(form)_4$ (0.15 g, 0.13 mmol) in $CHCl_3$ was allowed to react with crude AgO_2CCF_3 (30.2 mg, 0.13 mmol).

*Authors to whom correspondence should be addressed.

0020-1693/92/$5.00

After 3 h the reddish solution was filtered through celite to remove silver metal and layered with n-heptane. After six days deep-red crystals of **1** were collected; yield 75%. *Anal.* Found; C, 60.88; H, 4.99; N, 8.58; F, 4.88. Calc. for $C_{62}H_{62}N_8F_3O_3Rh_2$: C, 60.54; H, 5.08; N, 8.40; F, 4.63%.

Synthesis of [Rh₂(form)₄]NO₃ (2)

0.15 g (0.13 mmol) of $Rh_2(form)_4$ in $CHCl_3$ was allowed to react with solid $AgNO_3$ (23.2 mg, 0.13 mmol). Work-up as before gave complex **2** in 71%. *Anal.* Found: C, 55.89; H, 4.82; N, 9.40; O, 3.31. Calc. for $C_{60}H_{60}N_9O_3Rh_2 \cdot 1.5CHCl_3$: C, 55.12; H, 4.62; N, 9.40; O, 3.58%.

X-ray data collection and structure refinement

Suitable red–black crystals of **1** were obtained by slow evaporation of solvent from benzene–heptane solution. Diffraction measurements were made on a Siemens-Stoe four-circle diffractometer using graphite-monochromated Mo Kα ($\lambda = 0.71073$ Å) radiation. Accurate unit-cell dimensions and crystal orientation matrices were obtained from least-squares refinement of 25 strong reflections in the range $15 < 2\theta < 26°$. Compound **1** crystallizes in the tetragonal *P4/ncc* space group, with $a = 14.101(2)$, $b = 14.101(2)$, $c = 29.235(3)$ Å, $V = 5813.0(4)$ Å^3, $Z = 4$ and $D_{calc} = 1.24$ g cm^{-3}. Lorentz and polarization corrections were applied to the intensity data but no absorption correction was made due to the low absorption coefficient ($\mu = 6.2$ cm^{-1}) and the fairly uniform dimensions of the crystals. The structure was solved by using standard Patterson methods, successive least-squares refinements and difference Fourier maps. The final residual for 122 variables refined against the 926 data for which $F^2 > 3\sigma(F^2)$ were $R = 4.8\%$, $R_w = 6.8\%$. During the refinement it became apparent that a disordered trifluoroacetate anion was present around the fourfold axis. Several attempts to model this portion of the structure were made. The four highest areas of electron density, which constitute a reasonable bonding pattern for CF_3COO group, were assigned with an occupancy consistent with the site symmetry and isotropically refined. Scattering factors for non-hydrogen atoms were taken from ref. 4 and for hydrogen atoms from ref. 5. Anomalous dispersion corrections for Rh and Ag atoms were taken from ref. 6. All calculations were performed with SHELX76 [7] and PARST [8] set of programs on the IBM 4090/120S computer at the 'Centro di Calcolo dell'Università di Messina'.

Results and discussion

The synthesis of the complexes was easily accomplished in dichloromethane solution by oxidizing the Rh_2^{4+} complex $Rh_2(form)_4$ with the appropriate silver salt. It is clear evident that the nature of the counterion does not play any role in determining the nature of the products very likely owing to the steric demand of the tolyl groups which do not allow axial coordination. The oxidation reactions are very rapid and characterized by the formation of a grey precipitate of metallic silver. The IR spectra of the complexes in the 1500–1700 cm^{-1} region are dominated by two bands at 1520 and 1700 cm^{-1} due to form and uncoordinated trifluoroacetate groups, respectively. The complexes, which are 1:1 electrolytes, are quite stable in solution as in solid and the same products are obtained regardless of whether the oxidation is carried out in molar ratio 1:1 or 1:2 indicating that silver ions do not allow the thermodynamic access to dirhodium(III,III) derivatives. This is in agreement with the second oxidation of the starting complex which occurs at +1.06 V versus SCE in CH_2Cl_2. These values are much too high for Ag^+ ions to achieve. Complexes **1** and **2** react with carbon monoxide giving adducts stable as solids which show the ν(CO) at 2070 cm^{-1}, namely 30 cm^{-1} higher than

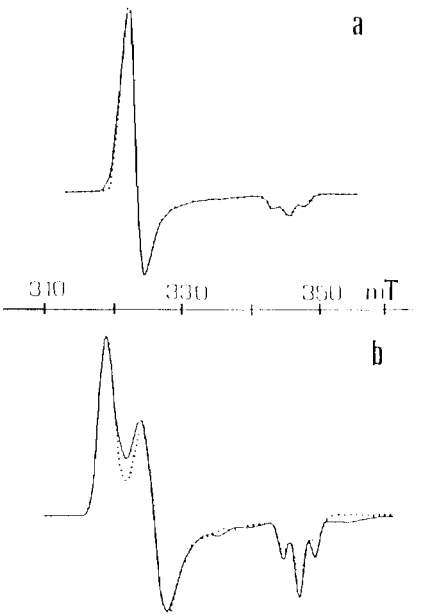

Fig. 1. Experimental (– – –) and best fit computer simulated (· · · · ·) EPR spectra of complex **1** (a) and **2** (b) detected at 100 K by using MeTHF as a solvent.

TABLE 1. Best fitting values of the g tensor components ($g_1 > g_2 > g_{\parallel}$) and of the rhodium nuclei hyperfine tensor principal components A_i (in units of 10^{-4} cm^{-1}) as obtained by computer simulation for compounds **1** and **2**; estimated error values of g_i and A_i are $\pm 2.10^{-3}$ and $\pm 1.10^{-4}$, respectively

Compound	g_1	g_2	$g_{\parallel}$	A_1	A_2	$A_{\parallel}$
1	2.078	2.073	1.958	10	12	17
2	2.105	2.061	1.934	10	12	17

that of the parent complex indicating an increase of the formal oxidation state of the metal centres.

The paramagnetic nature of the complexes obtained is reflected by their EPR spectra recorded in dichloromethane or methyltetrahydrofuran solution both at room temperature and at 100 K. The spectra of frozen solutions of the radical $[Rh_2(form)_4]^{\cdot+}$ show features similar to those of the samples electrochemically obtained [3]. At room temperature the EPR spectra consist of a sharp single line absorption centred at $g_{iso}=2.037$ (linewidth 2.5 mT). The sharp single line absorption is characteristic of a paramagnetic species whose structural anisotropies of g and hyperfine (A) tensors are completely averaged out by fast molecular tumbling motion. The EPR spectra recorded at 100 K consist of two or three absorption lines (Fig. 1); the low-field one (or two) is unresolved while that at high-field is split into three resonances with 1:2:1 relative intensities. This triplet structure can be easily interpreted on the basis of the hyperfine magnetic interaction between one electron and two ^{103}Rh nuclei ($I=1/2$). The spectrum was simulated by choosing the appropriate set of parameters for the principal values of g_i ($i=1,3$) of the g tensor and for those $A_i(i=1,3)$ of the hyperfine tensor. The EPR spectrum in frozen solution is interpreted as due to a paramagnetic system formed by two equivalent Rh nuclei and one delocalized electron and suggests that the complexes lie within the 'Class III' Robin–Day mixed-valent species [9] with non-integral oxidation state.

When the g_1 and g_2 values are fairly close together (Table 1) the low-field absorption lines collapse into a single line. The high-field pattern displays a resolved hyperfine structure because of the large value of the hyperfine component A_3 in the spin Hamiltonian of the Rh...Rh system. The hyperfine structure of the low-field line absorptions is not resolved, although computer simulation has allowed us to obtain an accurate evaluation of A_1 and A_2 hyperfine components.

We have noted that the EPR spectra of the examined products recorded in frozen solution exhibit spectral features that differ from those observed in the solid powder. In particular, in the latter case the triplet structure of the high-field line absorption disappears and a sharp single line merges. The difference in the two EPR spectra is attributed to the presence of anisotropic exchange interaction between neighbour paramagnetic centres that averages out the hyperfine structure. Therefore, the analysis of solid power EPR spectra in these compounds gives an incorrect evaluation of the magnetic parameters.

TABLE 2. Crystal and refinement data

Formula	$C_{62}H_{62}F_3N_8O_3Rh_2$
Formula weight	1230.04
Crystal system	tetragonal
Space group	*P4/ncc*
a (Å)	14.101(2)
b (Å)	14.101(2)
c (Å)	29.235(3)
V (Å^3)	5813.0
Z	4
ρcalc (g cm^{-3})	1.24
Crystal size (mm)	$0.08\times0.10\times0.07$
Orientation reflections: no., range (2θ)	25, $14<2\theta<26$
T (°C)	22
μ (cm^{-1})	6.2
Radiation (Å)	Mo Kα, $\lambda=0.71073$
Monochromator	graphite crystal
Scan type	θ–2θ
Scan speed	variable
Scan range, (°)	1.2
Standard reflections	3 measured after every 120′
Data limits	$3<2\theta<50$
No. data collected	1580
Observed data	926 ($I\geqslant3\sigma(I)$)
No. parameters refined	122
R[a]	0.048
R_w[b]	0.060
Weighting scheme	$w=0.1795/(\sigma^2(F_o)+0.011166F_o^2)$
Largest shift e.s.d. in final cycle	0.83
Largest peak (e/Å^3)	0.51

[a] $R=[\Sigma\|F_o\|-\|F_c\|]/\Sigma\|F_o\|$. [b] $R_w[\Sigma w(\|F_o\|-\|F_c\|)^2/\Sigma w\|F_o\|^2]^{1/2}$, $w=n/(\sigma^2(F_o))$.

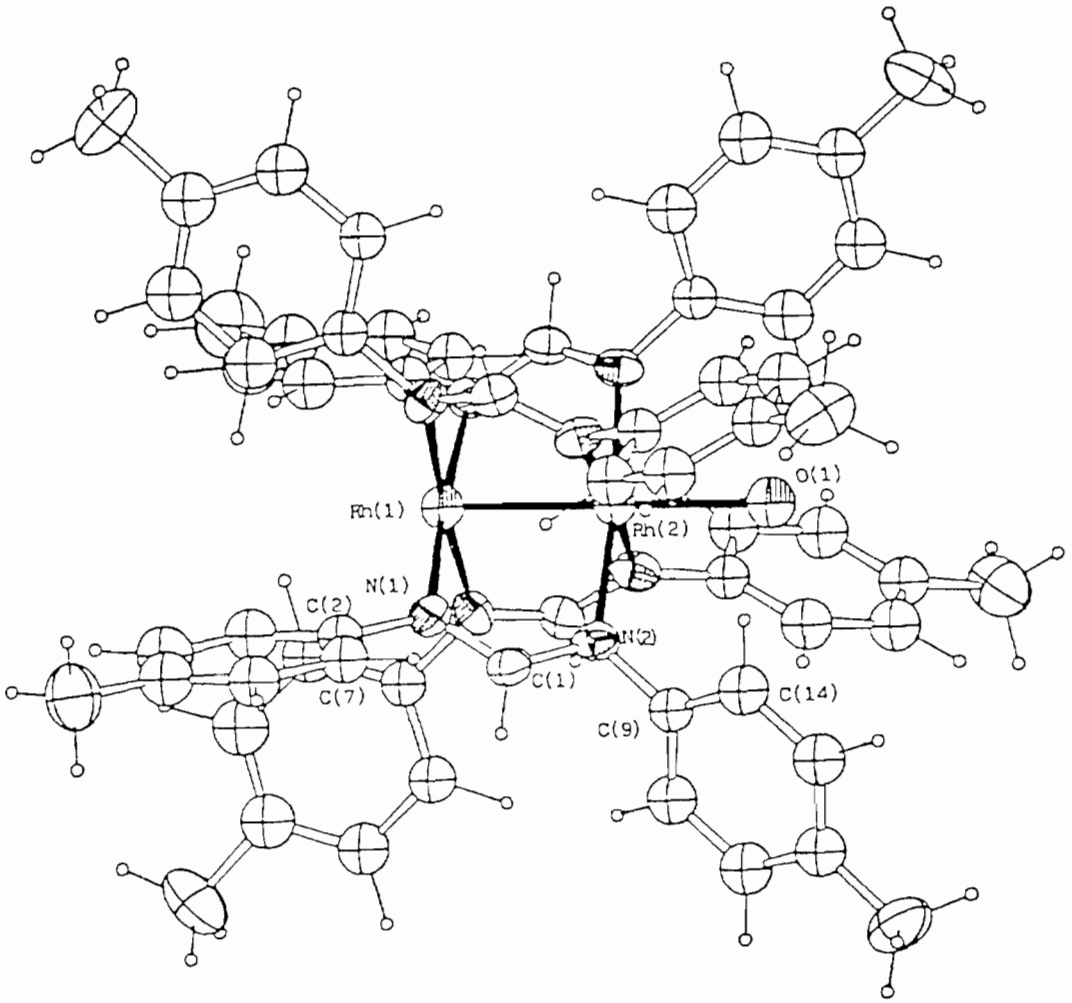

Fig. 2. An ORTEP view of the $[Rh_2(form)_4(H_2O)]^+$ cation showing 40% probability thermal ellipsoids.

All the complexes show characteristically a value of the g_3 component lower than $g_e(=2.0023)$ of the free electron, suggesting that the radical species here reported have the odd electron accommodated in a δ^*(RhRh) orbital. This suggestion is based on recent calculations of g tensor components in similar compounds carried out by Kawamura *et al.* [10] who have shown that an unpaired electron in a δ^*(RhRh) orbital causes a negative deviation of the g_3 component from the g_e value, while the same shift is positive when the odd electron is described by a π^*(RhRh) orbital.

The crystal structure of **1** (Table 2) consists of a discrete $[Rh_2(form)_4]^+$ cation with one molecule of water located at the Rh(2) axial position (Fig. 2), and one uncoordinated CF_3COO group disordered around the fourfold axis. Notwithstanding the disorder the model was well refined ($R=0.048$, $R_w=0.060$). The most salient features of this crystallographic analysis (Tables 3 and 4) are the lengthening of the Rh–Rh bond distance (2.452(2) Å), slightly longer than that of the neutral derivative [3], and the large difference between the Rh(2)–N(2)–C(9)–C(14) (63.2°) and Rh(1)–N(1)–C(2)–C(7) (38.5°) torsion angles (43.3° in the neutral species). This difference causes the loss of the crystallographic symmetry present in the neutral species {42 (D4)}. Furthermore the orientation of the tolyl group attached to N(2) avoids the unfavourable intramolecular contacts that in the parent complex prevent the coordination of water molecules. The length of the Rh–Ow bond (2.165(2) Å) is shorter than the normal value found in similar compounds while the Rh–Rh–Ow bond angle is 180°. The N–Rh–Rh–N torsion angle (18.1(3)°) lies close to the value found in the neutral derivative (16.7(2)°) while the other bond distances and angles fall in the typical range observed for other formamidinate derivatives and do not require special comments.

The most interesting point that emerges from the comparison of the structural data of complex **1** with those of the parent complex is that the oxidation results in lengthening of the Rh–Rh bond distance rather than shortening as expected on simple MO

TABLE 3. Bond distances (Å) and angles (°) for complex **1**

Distances			
Rh(2)–O(1)	2.165(2)	Rh(1)–N(1)	2.035(9)
Rh(1)–Rh(2)	2.452(2)	N(1)–C(1)	1.32(1)
Rh(2)–N(2)	2.050(8)	N(2)–C(1)	1.31(2)
N(1)–C(2)	1.42(2)	C(2)–C(3)	1.37(2)
N(2)–C(9)	1.40(1)	C(3)–C(4)	1.42(2)
C(2)–C(7)	1.35(2)	C(5)–C(6)	1.35(2)
C(4)–C(5)	1.36(2)	C(6)–C(7)	1.39(2)
C(5)–C(8)	1.52(2)	C(9)–C(14)	1.33(2)
C(9)–C(10)	1.39(2)	C(11)–C(12)	1.35(2)
C(10)–C(11)	1.39(2)	C(12)–C(15)	1.48(2)
C(12)–C(13)	1.37(2)	C(13)–C(14)	1.39(2)
Angles			
Rh(2)–Rh(1)–N(1)	87.3(3)	Rh(2)–Rh(1)–O(1)	180
Rh(1)–Rh(2)–N(2)	87.2(3)	Rh(1)–N(1)–C(2)	124.2(7)
Rh(1)–N(1)–C(1)	116.8(8)	C(1)–N(1)–C(2)	119.0(9)
Rh(2)–N(2)–C(9)	125.5(7)	Rh(2)–N(2)–C(1)	116.9(7)
C(1)–N(2)–C(9)	117.6(9)	N(1)–C(1)–N(2)	126(1)
N(1)–C(2)–C(7)	121(1)	N(1)–C(2)–C(3)	119(1)
C(3)–C(2)–C(7)	120(1)	C(2)–C(3)–C(4)	120(1)
C(3)–C(4)–C(5)	121(1)	C(4)–C(5)–C(8)	118(1)
C(4)–C(5)–C(6)	117(1)	C(6)–C(5)–C(8)	125(1)
C(5)–C(6)–C(7)	123(1)	C(2)–C(7)–C(6)	119(1)
N(2)–C(9)–C(14)	123(1)	N(2)–C(9)–C(10)	117(1)
C(10)–C(9)–C(14)	120(1)	C(9)–C(10)–C(11)	118(1)
C(10)–C(11)–C(12)	124(1)	C(11)–C(12)–C(15)	124(1)
C(11)–C(12)–C(13)	115(1)	C(13)–C(12)–C(15)	121(1)
C(12)–C(13)–C(14)	123(1)	C(9)–C(14)–C(13)	119(1)

TABLE 4. Fractional atomic coordinates for complex **1**

Atom	*x*	*y*	*z*
Rh(1)	0.000000	0.500000	0.16072(5)
Rh(2)	0.000000	0.500000	0.24458(6)
O(1)	0.500000	0.000000	0.1819(6)
N(1)	0.0973(7)	0.3936(7)	0.1640(3)
N(2)	0.1266(6)	0.4290(6)	0.2411(3)
C(1)	0.1463(7)	0.3860(8)	0.2025(4)
C(2)	0.1135(8)	0.3268(9)	0.1283(4)
C(3)	0.1286(8)	0.2337(8)	0.1393(4)
C(4)	0.1456(9)	0.1669(9)	0.1039(5)
C(5)	0.1436(9)	0.194(1)	0.0592(4)
C(6)	0.126(1)	0.286(1)	0.0501(5)
C(7)	0.1116(9)	0.3535(9)	0.0839(5)
C(8)	0.157(1)	0.117(1)	0.0231(6)
C(9)	0.1918(8)	0.4194(8)	0.2771(4)
C(10)	0.280(1)	0.4620(9)	0.2718(4)
C(11)	0.346(1)	0.452(1)	0.3068(4)
C(12)	0.3286(9)	0.4058(9)	0.3462(4)
C(13)	0.2393(9)	0.3688(9)	0.3502(5)
C(14)	0.1711(9)	0.3747(9)	0.3158(5)
C(15)	0.400(1)	0.396(1)	0.3834(6)
C(70)	0.500000	0.000000	0.008(2)
C(71)	0.000000	0.500000	0.435(5)
O(2)	0.518(3)	0.085(3)	0.095(1)
F(1)	0.521(4)	0.100(3)	0.031(1)

grounds. For example the oxidation of the complex $Rh_2(O_2CCH_3)_4(H_2O)_2$ [11] causes appreciable shortening of the Rh–Rh, Rh–O(eq) and Rh–O(H_2O) bond distances. The same correlation order bond/bond length has also been found for the couples $[Rh_2(Bridge)_4(L)_2]^{0/1+}$ (Bridge = acetate, acetamidate, trifluoroacetamidate; L = $AsPh_3$, $SbPh_3$) by resonance Raman spectra which show that ν(Rh–Rh) for the neutral derivative falls at lower frequencies than those of the corresponding radical species [12]. On the contrary the couple $[Rh_2(dpf)_4CH_3CN]^{0/1+}$ (dpf = diphenylformamidinate) shows a different correlation order bond/bond length and the length of the metal–metal bond increases on oxidation by 0.0021 Å [13]. Other couples such as $Rh_2(NHCOMe)_4(H_2O)_2$/$[Rh_2(NHCOMe)_4(Theophilline)_2]^+$ [14] and $Rh_2(Apy)_4$/$Rh_2(Apy)_4Cl$ (Apy = anylinopyridine) [15] are not useful when discussing Rh–Rh bond distance changes because it is essential that the comparison is made between compounds with identical axial ligands.

Concerning the couple $Rh_2(form)_4$/$[Rh_2(form)_4(H_2O)]^{1+}$ the counter-intuitive bond lengthening cannot be explained in terms of ligand-centred MO oxidation as found for example for the complex $Pd_2(form)_4$ [16]. On the other hand we cannot make unwarranted comparisons between the neutral and radical species because of the presence of axial water in **1**. However we believe that the *trans* effect of the axial water cannot counteract the strengthening of the Rh–Rh bond arising from a formal bond order of 1.5 and cannot be the only cause of the lengthening of the Rh–Rh bond in **1**.

In conclusion the relationship between order bond and metal–metal bond distance for Rh_2^{4+}/Rh_2^{5+} couples remains an open question because the understanding of the factors which determine the above correlation is at the present time severely hampered from the paucity of X-ray analyses of homologous Rh_2^{4+}/Rh_2^{5+} couples as well as by contrasting results.

We are continuing studies directed toward the synthesis and structural characterization of other Rh_2^{5+} formamidinate derivatives containing coordinating anions at the axial position.

Supplementary material

Hydrogen atom coordinates, thermal parameters, and tables of observed and calculated structure factors are available on request from the authors.

Acknowledgement

Financial support for this study from the Ministero della Pubblica Istruzione (Rome) is gratefully acknowledged.

References

1 G. A. Rizzi, M. Casarin, E. Tondello, P. Piraino and G. Granozzi, *Inorg. Chem., 26* (1987) 3406.
2 P. Piraino, G. Bruno, G. Tresoldi, S. Lo Schiavo and P. Zanello, *Inorg. Chem., 26* (1987) 91.
3 P. Piraino, G. Bruno, S. Lo Schiavo, F. Laschi and P. Zanello, *Inorg. Chem., 26* (1987) 2205.
4 D. T. Cromer and J. B. Mann, *Acta Crystallogr., Sect. A, 24* (1968) 321.
5 R. F. Stewart, *J. Chem. Phys., 53* (1970) 3175.
6 *International Tables for X-ray Crystallography,* Vol. IV, Kynoch, Birmingham, UK, 1974.
7 G. M. Sheldrick, *System of Computing Programs,* University of Cambridge, UK, 1976.
8 M. Nardelli, *Comput. Chem., 7* (1983) 95.
9 M. B. Robin and P. Day, *Adv. Inorg. Chem. Radiochem., 10* (1967) 247.
10 T. Kawamura, K. Fukamachi, T. Sowa, S. Hayashida and T. Yonezawa, *J. Am. Chem. Soc., 103* (1981) 364.
11 J. J. Ziolkowski, M. Moszner and T. Glowiak, *J. Chem. Soc., Chem. Commun.,* (1977) 760.
12 J. P. Best, R. J. H. Clark and A. J. Nightingale, *Inorg. Chem., 29* (1990) 1383.
13 J. L. Bear, C. L. Yao, R. S. Lifsey, J. D. Korp and K. M. Kadish, *Inorg. Chem., 30* (1991) 336.
14 K. Aoki, M. Hoshino, T. Okada, H. Yamazaki and H. Sekizawa, *J. Chem. Soc., Chem. Commun.,* (1986) 314.
15 J. L. Bear, C. L. Yao, L. M. Liu, F. J. Capdevielle, J. D. Korp, T. A. Albrigt, S. K. Kang and K. M. Kadish, *Inorg. Chem., 28* (1989) 1254.
16 F. A. Cotton, M. Matusz, R. Poli and X. Feng, *J. Am. Chem. Soc., 110* (1988) 1144.